Title

Optothermally Assembled Nanostructures.

Journal

Accounts of materials research, 2(5)

Authors

Li, Jingang
Zheng, Yuebing

Publication Date

2021-05-28

DOI

10.1021/accountsmr.1c00033

Peer reviewed

HHS Public Access

Author manuscript

Acc Mater Res. Author manuscript; available in PMC 2022 May 28.

Published in final edited form as:

Acc Mater Res. 2021 May 28; 2(5): 352–363. doi:10.1021/accountsmr.1c00033.

Optothermally Assembled Nanostructures

Jingang Li,

Materials Science & Engineering Program, Texas Materials Institute, and Walker Department of Mechanical Engineering, The University of Texas at Austin, Austin, Texas 78712, United States

Yuebing Zheng

Materials Science & Engineering Program, Texas Materials Institute, and Walker Department of Mechanical Engineering, The University of Texas at Austin, Austin, Texas 78712, United States

CONSPECTUS:

Nanofabrication is one of the core techniques in rapidly evolving nanoscience and nanotechnology. Conventional top-down nanofabrication approaches such as photolithography and electron beam lithography can produce high-resolution nanostructures in a robust way. However, these methods usually involve multistep processing and sophisticated instruments and have difficulty in fabricating three-dimensional complex structures of multiple materials and reconfigurability. Recently, bottom-up techniques have emerged as promising alternatives to fabricating nanostructures via the assembly of individual building blocks. In comparison to top-down lithographical methods, bottom-up assembly features the on-demand construction of superstructures with controllable configurations at single-particle resolution. The size, shape, and composition of chemically synthesized building blocks can also be precisely tailored down to the atomic scale to fabricate multimaterial architectural structures of high flexibility. Many techniques have been reported to assemble individual nanoparticles into complex structures, such as self-assembly, DNA nanotechnology, patchy colloids, and optically controlled assembly. Among them, the optically controlled assembly has the advantages of remote control, site-specific manipulation of single components, applicability to a wide range of building blocks, and arbitrary configurations of the assembled structures.

In this Account, we provide a concise review of our contributions to the optical assembly of architectural materials and structures using discrete nanoparticles as the building blocks. By exploiting entropically favorable optothermal conversion and controlling optothermal−matter interactions, we have developed optothermal assembly techniques to manipulate and assemble individual nanoparticles. Our techniques can be operated both in solution and on solid substrates. First, we discuss the opto-thermoelectric assembly (OTA) of colloidal particles into superstructures by coordinating thermophoresis and interparticle depletion bonding in the solution. Localized laser heating generates a temperature gradient field, where the thermal migration of ions creates a thermoelectric field to trap charged particles. The depletion of ion species at the gap

Corresponding Author: Yuebing Zheng – Materials Science & Engineering Program, Texas Materials Institute, and Walker Department of Mechanical Engineering, The University of Texas at Austin, Austin, Texas 78712, United States; zheng@austin.utexas.edu.

Complete contact information is available at: https://pubs.acs.org/10.1021/accountsmr.1c00033

The authors declare no competing financial interest.

between closely positioned particles under optical heating provides strong interparticle bonding to stabilize colloidal superstructures with precisely controlled configurations and interparticle distances. Second, we discuss bubble-pen lithography (BPL) for the rapid printing of nanoparticles using an optothermal microbubble. The long-range convection flow induced by the optothermal bubble drags the colloidal particles to the substrate with a high velocity. BPL represents a general method for printing all kinds of building blocks into desired patterns in a high-resolution and high-throughput way. Third, we present the optothermally-gated photon nudging (OPN) technique, which manipulates and assembles particles on a solid substrate. Our solid-phase optical control of particles synergizes the modulation of particle−substrate interactions by optothermal effects and photon nudging of the particles by optical scattering forces. Operated on the solid surfaces without liquid media, OPN can avoid the undesired Brownian motion of nanoparticles in solutions to manipulate individual particles with high accuracy. In addition, the assembled structures can be actively reassembled into new configurations for the fabrication of tunable functional devices. Next, we discuss applications of the optothermally assembled nanostructures in surface-enhanced Raman spectroscopy, color displays, biomolecule sensing, and fundamental research. Finally, we conclude this Account with our perspectives on the challenges, opportunities, and future directions in the development and application of optothermal assembly.

Graphical Abstract

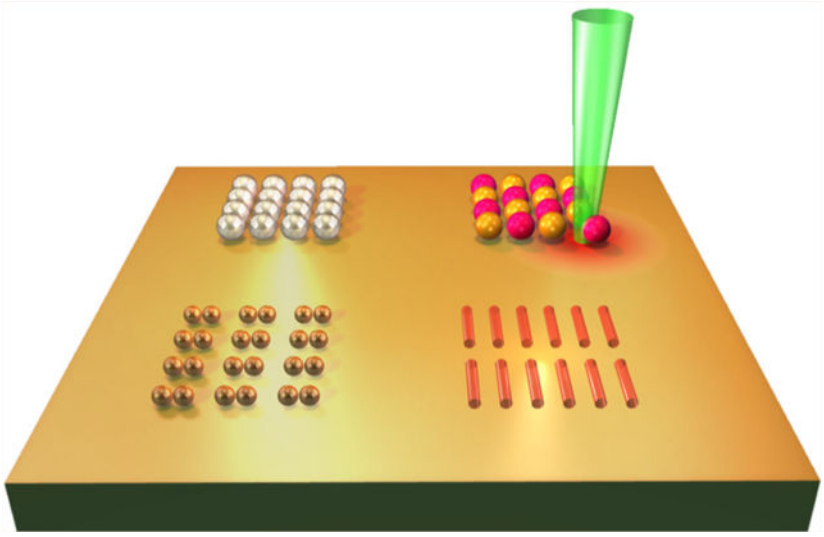

1. INTRODUCTION

Bottom-up assembly techniques have attracted significant research interest for the fabrication of functional nanostructures.[1,2] Compared with traditional top-down lithographical approaches such as photolithography and electron beam lithography, bottom-up assembly is promising to create complex multimaterial structures with precisely controlled configurations at single-particle resolution.[3,4] Many bottom-up assembly approaches also feature low-cost, simple equipment, single-step processing, and a low waste of materials. Mean-while, chemical synthesis techniques can produce colloidal building blocks with precisely tunable sizes, shapes, and compositions down to the atomic scale

(Figure 1),[5] which enhances flexibility in the assembly of variable complex superstructures. The intercomponent coupling in the assembled structures can also lead to improved or new properties beyond individual components.[6] Self-assembly offers an autonomous way to build colloidal particles into large-scale structures.[7,8] However, it is usually restricted to thermodynamically stable structures.

Many approaches were developed to extend the capability of self-assembly to fabricate nanostructures with more complex configurations. For instance, template-assisted self-assembly can create functional structures with accurate configurations that are predefined by the template.[9,10] Alternatively, the regioselective modification of colloidal particles with organic or biological molecules (e.g., copolymer and DNA) allows interparticle directional bonding for the programmable self-assembly of diverse superstructures.[11,12] In addition, the directed motion of colloids under electric[13] and magnetic[14,15] fields has been harnessed to assemble large ensembles of colloidal structures. However, these field-directed self-assembly techniques require a sophisticated design of the colloidal systems and experimental setups, which are also limited to specific assembly configurations and colloidal particles that are responsive to electric or magnetic fields.

Assembling colloidal superstructures with arbitrary configurations requires the precise manipulation and positioning of individual colloidal building blocks. Optical assembly is highly promising for this purpose because it allows remote and site-specific control of single components to assemble the components into superstructures with any desired configuration. For instance, the targeted assembly of phototactic microswimmers was demonstrated under light illumination.[16] Optical tweezers are capable of manipulating colloidal particles of variable sizes and materials in a versatile manner.[17] However, it has remained challenging for conventional optical tweezers to efficiently assemble colloidal superstructures.[18] This is because the development of any optical assembly technique into a nanomanufacturing tool requires both the precise manipulation of individual colloidal particles and the rational control of interparticle and particle–substrate interactions. While conventional optical tweezers lack control of the interparticle and particle–substrate interactions, optothermal manipulation techniques exploiting entropically favorable optothermal–matter coupling are promising for controlling these interactions for the targeted assembly of colloidal structures. This Account summarizes our recent progress in the development of a series of optothermal assembly techniques for the on-demand assembly of diverse nanostructures. We also discuss the applications of the assembled structures and provide our prospects on the emerging field of optothermal assembly.

2. OPTOTHERMAL ASSEMBLY TECHNIQUES

2.1. Opto-thermoelectric Assembly

Opto-thermoelectric assembly (OTA) is realized by trapping and assembling colloidal particles one by one in a light-generated temperature gradient field.[19–21] To enable opto-thermoelectric trapping of diverse colloidal particles, a cationic surfactant, cetyltrimethylammonium chloride (CTAC), was added to the solution to create a thermoelectric field.[22] A plasmonic substrate consisting of quasi-continuous gold nanoislands was used to efficiently create a temperature gradient field under localized laser

heating.[23] Briefly, both CTAC micelles and Cl^- ions moved away from the laser beam to the cold region under the temperature gradient field.[24] The differences in Soret coefficients (i.e., $S_T(\text{micelles}) \gg S_T(Cl^-)$) induced a spatial separation of positive CTAC micelles and negative Cl^- ions, which created an electric field pointing toward the laser beam.[25] Therefore, CTAC-modified particles with positive charge were trapped at the laser beam by the thermoelectric forces (Figure 2a).[22] It should be noted that CTAC can be replaced by other surfactants with similar thermophoretic responses such as poly(diallyldimethyl-ammonium chloride). By translating the laser beam or substrate, we managed to transport the trapped particle (Figure 2b) to any targeted location (Figure 2c).

Opto-thermoelectric tweezers can trap particles with an optical intensity of 0.05–0.4 mW μm^{-2} that is 2 to 3 orders of magnitude lower than the typical laser intensity in optical tweezers (10–100 mW μm^{-2}), thus providing a noninvasive tool to handle the building blocks for colloidal assembly. The general strategy of surface charge modification makes it a universal technique for trapping all kinds of colloidal particles. In addition, our integrated optical spectroscopy allows in situ characterization of the optical properties of the particles to reveal their size, shape, and composition for the precise assembly of multiscale and multicomponent structures (Figure 2b). By integrating opto-thermoelectric tweezers with a digital micromirror device, we have demonstrated the highly efficient parallel trapping and manipulation of multiple colloidal particles of different materials and sizes (Figures 2d,e).

The addition of CTAC to the solution not only creates the thermoelectric field for the trapping and manipulation of particles but also provides the interparticle bonding for OTA. When two particles are trapped at the laser beam, thermophoresis drives CTAC micelles out of the interparticle gap, leading to a depletion force between two connected particles (Figure 3a).[26] This interparticle bonding is highly tunable depending on the CTAC concentration, which can be maintained even after the temperature field is off, making it possible to assemble colloidal matter with tunable interparticle bonding in the solution. By using colloidal particles of different materials, shapes, and sizes as the building blocks, we demonstrated the capability of OTA to assemble complex superstructures.[26] Figure 3b–d shows the hybrid assembly of a one-dimensional (1D) chain, a two-dimensional (2D) lattice, and a 2D Saturn-ring structure using PS beads with different sizes, respectively. The assembly of anisotropic particles was also demonstrated with precise orientational control (Figure 3e). The OTA strategy can be widely applied to various materials. For instance, we demonstrated the assembly of a PS/SiO_2 heterogeneous lattice (Figure 3g) and the PS/Au dimer structure (Figure 3h). By incorporating optical scattering forces for the out-of-plane control of colloidal particles, we further showed the assembly of three-dimensional (3D) structures using OTA (Figure 3f). OTA was also used to assemble the larger-area patterns with precisely controlled configurations by assembling individual colloidal particles one by one (Figure 3i).

Although OTA permits the assembly of diverse colloidal matter in solution, the immobilization of these assembled structures onto solid substrates, which is essential to the implementation of on-chip devices, remains a challenge.[27] We have proposed two approaches to overcome this challenge. One is that, by assembling colloidal structures in a photocurable hydrogel solution, we demonstrated the immobilization of colloidal structures

through the localized cross-linking of hydrogels with ultraviolet irradiation (Figure 4a).[28] In this way, the assembled patterns could remain intact even after the samples were rinsed and dried (Figure 4b). The second strategy is to print the particle onto the substrate via the depletion attraction between the substrate and the particles.[29] Similar to the interparticle bonding in OTA, the depletion of CTAC micelles at the particle–substrate gap leads to an adhesion force that can bind the particle to the substrate (Figure 4c). Interestingly, by centering the laser beam on the printed particle, we can drive back CTAC micelles into the particle–substrate gap to release the printed particle back into the solution due to the repulsive electrostatic force between CTAC micelles and the CTAC-coated particle (Figure 4d). As a demonstration, we achieved the reconfigurable printing of particle arrays from a "sad-face" pattern to a "smiley-face" pattern by releasing and reprinting one particle within the arrays (Figure 4e).

2.2. Bubble-Pen Lithography

Optothermal microbubbles can be generated by localized optical heating in the solution[30,31] and have been used to trap and manipulate colloidal particles.[32–34] We developed bubble-pen lithography (BPL) as a versatile optical printing technique using a microbubble as the micropen (Figure 5a).[35] The microbubble is generated by the plasmon-enhanced optical heating when a laser beam is directed onto the plasmonic substrate. The Marangoni convection flow induced by the microbubble drives particles toward the bubble surface (Figure 5b), where particles are then immobilized on the substrate by van der Waals interactions. The diameter of the microbubble can be precisely controlled by tuning the optical density. Particles with a wide range of sizes can be printed (Figure 5c), which is desired for printing multiscale structures. By steering the laser beam and controlling the on/off state of the laser, BPL can realize both the one-by-one assembly of single particles into arbitrary patterns (Figure 5d) and the continuous writing of particle assemblies (Figure 5e,f). It should be mentioned that the line width of particle assemblies during continuous printing can be well-controlled by the laser power (Figure 5g), which allows easy modulation of the printed patterns.

We further demonstrated the use of BPL for the high-throughput printing of quantum dots (QDs).[36] Arbitrary patterns consisting of QD assemblies can be created by the programmable translational motion of the stage that holds the substrate in an optical microscope. We achieved a printing speed of up to 1 cm/s, which was limited by the stage motion speed (Figure 6a). This printing speed can be further improved with advanced motorized stages or fast-scanned laser beams. Figure 6b shows the printing of a large-area pattern, where the fluorescence lifetime mapping shows the uniform deposition of QDs. We further integrated BPL with a smartphone to develop haptic-interfaced BPL for the facile control of QD printing (Figure 6c).[37] Free-form printing of QDs can be achieved by simply drawing the desired patterns on the smartphone (Figure 6d). In addition, the printing scale and speed can be preset by the smartphone for versatile control of the printed structure (Figure 6e).

Besides printing the preformed colloidal particles and quantum dots, BPL also provides a powerful platform for directing in situ synthesis and the subsequent assembly of metallic

nanostructures. For instance, we have demonstrated the bubble-mediated fabrication of silver ring nanostructures[38] and metal alloy nanoparticles[39] directly from the precursor solutions.

2.3. Optothermally-Gated Photon Nudging

The manipulation and assembly of particles are mostly operated in fluidic environments. However, to assemble stable colloidal nanostructures, liquid-phase operation suffers from undesired pattern collapses and the Brownian motion of nanoparticles. To address these limitations, we proposed solid-phase optical manipulation with optothermally-gated photon nudging (OPN) (Figure 7a).[40] In comparison to the particle manipulations in the liquid environment, manipulating particles on the solid substrate needs to overcome the much stronger van der Waals friction forces at the solid–solid interfaces.[41] In our case, we solved this issue by introducing a thermoresponsive layer to reduce the friction forces by modulating the particle–substrate interactions. Briefly, a solid CATC layer is introduced between the particles and the substrate, acting as an optothermal gate. At room temperature, the CTAC remains at its solid phase to bind particles with van der Waals forces. After the laser is turned on, the optical heating of colloidal particles leads to a localized phase transition of CTAC from the solid phase to a quasi-liquid structure (Figure 7b). In this way, the resistant friction forces between particles and the substrate is significantly reduced, and particles can be nudged by optical scattering forces simultaneously. By translating the laser beam or the substrate, particles can be manipulated to any target location. OPN is generally applicable to a wide range of materials that interact strongly with light, including metals, semiconductors, dielectrics, and metal oxides. As a solid-phase technique, OPN can effectively avoid the Brownian motion of nanoparticles to achieve high-accuracy manipulation. For instance, we demonstrated the precise manipulation of nine randomly dispersed silicon nanoparticles into a 3 × 3 array with an average position error of ~200 nm (Figure 7c). Since OPN is operated on a solid substrate, it allows the dynamic manipulation of particles to new sites for the reconfigurable assembly of colloidal structures. As an example, four gold nanoparticles were sequentially assembled into an L-shaped pattern, a square, a mirrored L-shaped pattern, and a straight line (Figure 7d). We also demonstrated the reconfigurable assembly of metal–dielectric structures for functional on-chip devices. For instance, one gold nanowire and two silicon nanoparticles were arranged into a “Y” letter and then transformed to a “Z” letter by moving the particles and rotating the nanowire (Figure 7e).

3. APPLICATIONS OF OPTOTHERMALLY ASSEMBLED NANOSTRUCTURES

With the diversity in compositions, configurations, and properties, the assembled nanostructures can be applied to a broad range of applications. In this section, we discuss some of the applications enabled by optothermally assembled nanostructures.

First, we discuss the applications of closely assembled colloidal nanoparticles. Plasmonic nanostructures exhibit a strong electric-field enhancement to enable surface-enhanced Raman spectroscopy (SERS) for the detection of molecules at low concentrations.[42] We demonstrated that the plasmonic nanoparticle assemblies prepared by OTA are promising

candidates for in situ SERS detection of molecules in liquid environments (Figure 8a).[43] Numerous plasmonic hotspots are present in the metal nanoparticle assemblies, where the electric field enhancement can be further controlled by the CTAC concentration, the composition and geometry of the metal nanoparticles, and the size of the particle assemblies (Figure 8b). We have achieved a detection limit of 1 μM for rhodamine 6G using the 100 nm silver nanoparticle assemblies. In another example, the site-specific assembly of fluorescent QDs on the substrate by BPL can be used for microdisplay applications. We have demonstrated the regioselective printing of QDs with different emission colors on a single substrate (Figure 8c).[36] This multicolor printing was accomplished by a multistep process involving sequential supplies of the different QD inks. Alternatively, we established the fluorescence tuning of printed QDs via programmed control of printing speeds. During QD printing, laser heating can cause the photo-oxidation of printed QDs to reduce their effective size, leading to a spectral blue shift.[44] Thus, by tuning the printing speed to control the oxidation time, we demonstrated the printing of QDs with tunable fluorescent color from yellow to blue.[37] High-resolution printing of multicolor QDs makes BPL a promising technique for applications in full-color microdis-plays.

With their site-specific control of individual building blocks, optothermal assembly techniques allow us to precisely tune the structural configurations of assembled nanostructures to explore the new properties and establish the structure–property relationships. For instance, by mimicking the molecular structure of chiral molecules, we used OTA to assemble chiral meta-molecules using colloidal particles as the meta-atoms.[45] Individual particles dispersed in the solution were assembled into specific molecular structures, which could be disassembled and subsequently reassembled to their enantiomers with different handedness (Figure 8e). The differential scattering spectra of the left-handed (LH) and right-handed (RH) meta-molecules had a bisignate feature (Figure 8f), indicating the mirror symmetry between the enantiomers. Chiral metamolecules assembled by OTA provide a microscopic model for bridging molecular structures with optical chirality to understand the fundamental origin of chirality in the actual molecular and colloidal systems.[46,47] We also exploited OPN to assemble tunable chiral nanostructures on the solid substrate using a silicon nanoparticle and a silicon nanowire as the building blocks (Figure 8g).[48] The coexisting electric and magnetic resonances in the assembled dielectric nanostructures support the strong enhancement of optical near-field chirality for the detection and sensing of chiral molecules.[49,50] We demonstrated this chiral sensing capability using two enantiomers of phenylalanine as the sample analytes. The peak shifts of differential scattering spectra ($\Delta\lambda_{LH}$ and $\Delta\lambda_{RH}$ for LH and RH structures, respectively) induced by the adsorption of chiral molecules were measured to obtain the dissymmetric factor, $\Delta\Delta\lambda = \Delta\lambda_{LH} - \Delta\lambda_{RH}$ (Figure 8h). This factor reflects the structural chirality of the adsorbed molecules,[51] where $\Delta\Delta\lambda$ is positive (1.16 ± 0.47 nm) for D-phenylalanine and negative (−0.90 ± 0.44 nm) for L-phenylalanine (Figure 8i).

4. CONCLUSIONS AND OUTLOOK

As an entropically favorable process, light-to-heat conversion provides a convenient and efficient way to regulate the temperature field and optothermal–matter interactions for on-demand control of colloidal particles. In the liquid environment, regioselective optical

heating can create a temperature gradient field, where the motion of particles and other colloidal species can be controlled by thermophoresis. Localized optical heating in the solution can also create an optothermal microbubble for assembling and printing colloidal particles with bubble-mediated Marangoni flow. Alternatively, the optothermal effect can effectively modulate the particle–substrate interactions to enable the optical manipulation and assembly of nanostructures on solid substrates. With the diverse working mechanisms and operational environments, optothermal assembly techniques present a general platform for the versatile construction of colloidal nanostructures with complex architectures.

Table 1 summarizes the merits and limitations of the optothermal assembly techniques presented in this Account. Depending on the purpose of colloidal assembly, one can choose a specific technique for optimum performance. For instance, OTA is suitable for the assembly of colloidal matter in the solution with tunable bonding strengths, which is highly desired for the study of various couplings among colloidal particles and the development of tunable colloidal metamaterials. OPN is more capable of patterning nanostructures on the solid substrate for the fabrication of reconfigurable nanodevices. While OTA and OPN are more suitable for relatively small-scale colloidal assembly, BPL presents a high-throughput approach to printing colloidal inks into large-scale patterns for functional materials and devices. Herein, we further discuss challenges and potential directions for the future development of optothermal assembly techniques and their applications in architectural nanostructures.

First, as bottom-up techniques, optothermal assembly has the advantage of constructing architectural nanostructures at single-particle resolution. However, this feature also results in one of the most significant limitations of this method: low throughput. In comparison to top-down lithographic techniques that can define a large-scale pattern within seconds, optothermal assembly relies on the manipulation of single building blocks to build the superstructures, which is a relatively time-consuming process. To enhance the throughput of optothermal assembly, one could improve the efficiency in manipulating single colloidal particles by better understanding the manipulation mechanism and further optimizing the manipulation system. For instance, one can further optimize the laser wavelength, optics, and substrate quality in the OPN technique to achieve a more effective manipulation of colloidal particles on the solid substrate. An alternative way is to integrate a programmable spatial light modulator or digital micromirror device to achieve parallel control of multiple particles.[52] Additionally, the incorporation of microfluidics into the optothermal assembly platform will provide an efficient approach to the continuous and automated assembly of colloidal structures.

Second, optothermal assembly has mainly been applied to assemble 2D structures. Although OTA has demonstrated the capability of 3D assembly with simple configurations, the versatile assembly of complex 3D structures remains elusive. This limitation comes from the challenge of realizing a stable trapping potential along the out-of-plane direction (i.e., z axis in Figure 7b). We have recently developed two approaches to achieving a 3D optothermal manipulation of colloidal particles that can help to overcome this limitation. One method is to integrate the optothermal substrate into an optical fiber to achieve a 3D manipulation of particles via on-demand control over the laser focus along the z axis.[53] The other

approach uses the target particle as a self-heating source to achieve the manipulation along all directions without the need for an optothermal substrate.[54] Both methods can be extended to assemble more complex 3D structures. Other approaches to achieving a 3D optothermal assembly can involve the 3D engineering of the substrate and the integration of other forces, including optical forces and electric forces.[55–57]

Finally, with the versatile capability in the manipulation, assembly, and printing of diverse colloidal particles, optothermal assembly techniques are expected to stimulate more advances in a broad range of fields. They provide an ideal platform for studying colloidal sciences, materials science, and nanophotonics. For example, optothermal assembly can turn colloidal particles into nanostructures with tunable bonding strength and reconfigurable geometry. The easy integration of optical spectroscopy into the assembly system provides an effective tool for characterizing the optical properties and interparticle interactions in the assembled structures in situ. In addition, during the further development and optimization of optothermal assembly techniques, one will have tremendous opportunities to advance the fundamental understanding of colloidal sciences, surface chemistry, thermal science, photonics, and fluidics. Optothermal assembly techniques are also suitable for the fabrication of functional nanodevices with new functions and ultimate miniaturization. With their advantages of applicability to a wide range of materials, site-specific multicomponent fabrication, and low optical damage to nanomaterials, optothermal assembly techniques, once further developed, are promising for prototyping novel optical gratings,[58] optical waveguides,[59] optical circuits,[60] topological nanostructures,[61] and other photonic and electronic nanodevices.

ACKNOWLEDGMENTS

J.L. and Y.Z. acknowledge the financial support of the National Institute of General Medical Sciences of the National Institutes of Health (DP2GM128446) and the National Science Foundation (NSF-ECCS-2001650 and NSF-CMMI-1761743). J.L. also acknowledges the financial support of a University Graduate Continuing Fellowship from The University of Texas at Austin.

Biographies

Jingang Li is a Ph.D. candidate in Yuebing Zheng's group at The University of Texas at Austin. He received his B.Sc. in applied physics from the Special Class for the Gifted Young at the University of Science and Technology of China in 2017.

Yuebing Zheng is an associate professor of mechanical engineering and materials science & engineering at The University of Texas at Austin. He also holds the William W. Hagerty Fellowship in Engineering. He received his Ph.D. in engineering science and mechanics from The Pennsylvania State University in 2010. He was a postdoctoral researcher at The University of California, Los Angeles, from 2010 to 2013. His research group (http://zheng.engr.utexas.edu) engages in interdisciplinary research involving optics, materials science, chemistry, biology, engineering, and machine learning to innovate optical manipulation and measurement for the nanoscale, biological, and extraterrestrial world. He has been awarded the NIH Director's New Innovator Award, the NASA Early Career Faculty Award, the ONR Young Investigator Award, and the Beckman Young Investigator Award.

REFERENCES

(1). Shimomura M; Sawadaishi TBottom-up Strategy of Materials Fabrication: A New Trend in Nanotechnology of Soft Materials. Curr. Opin. Colloid Interface Sci2001, 6, 11–16.

(2). Zhang SBuilding from the Bottom Up. Mater. Today2003, 6, 20–27.

(3). Jin R; Zeng C; Zhou M; Chen YAtomically Precise Colloidal Metal Nanoclusters and Nanoparticles: Fundamentals and Opportunities. Chem. Rev2016, 116, 10346–10413. [PubMed: 27585252]

(4). Tan SJ; Campolongo MJ; Luo D; Cheng WBuilding Plasmonic Nanostructures with DNA. Nat. Nanotechnol2011, 6, 268–276. [PubMed: 21499251]

(5). Matijevic EProduction of Monodispersed Colloidal Particles. Annu. Rev. Mater. Sci1985, 15, 483–516.

(6). Wang W; Ramezani M; Väkeväinen AI; Törmä P; Rivas JG; Odom TWThe Rich Photonic World of Plasmonic Nanoparticle Arrays. Mater. Today2018, 21, 303–314.

(7). Whitesides GM; Grzybowski BSelf-Assembly at All Scales. Science2002, 295, 2418–2421. [PubMed: 11923529]

(8). Wang PY; Shields C. W. t.; Zhao T; Jami H; Lopez GP; Kingshott PRapid Self-Assembly of Shaped Microtiles into Large, Close-Packed Crystalline Monolayers on Solid Surfaces. Small2016, 12, 1309–1314. [PubMed: 26756607]

(9). Zhang M; Magagnosc DJ; Liberal I; Yu Y; Yun H; Yang H; Wu Y; Guo J; Chen W; Shin YJ; Stein A; Kikkawa JM; Engheta N; Gianola DS; Murray CB; Kagan CRHigh-Strength Magnetically Switchable Plasmonic Nanorods Assembled from a Binary Nanocrystal Mixture. Nat. Nanotechnol2017, 12, 228. [PubMed: 27819691]

(10). Greybush NJ; Saboktakin M; Ye X; Della Giovampaola C; Oh SJ; Berry NE; Engheta N; Murray CB; Kagan CRPlasmon-Enhanced Upconversion Luminescence in Single Nano-phosphor-Nanorod Heterodimers Formed through Template-Assisted Self-Assembly. ACS Nano2014, 8, 9482–9491. [PubMed: 25182662]

(11). Chen G; Gibson KJ; Liu D; Rees HC; Lee J-H; Xia W; Lin R; Xin HL; Gang O; Weizmann YRegioselective Surface Encoding of Nanoparticles for Programmable Self-Assembly. Nat. Mater2019, 18, 169–174. [PubMed: 30510268]

(12). Gong Z; Hueckel T; Yi GR; Sacanna SPatchy Particles Made by Colloidal Fusion. Nature2017, 550, 234–238. [PubMed: 28922664]

(13). Yan J; Han M; Zhang J; Xu C; Luijten E; Granick SReconfiguring Active Particles by Electrostatic imbalance. Nat. Mater2016, 15, 1095–1099. [PubMed: 27400388]

(14). Erb RM; Son HS; Samanta B; Rotello VM; Yellen BBMagnetic Assembly of Colloidal Superstructures with Multipole Symmetry. Nature2009, 457, 999–1002. [PubMed: 19225522]

(15). Yan J; Bae SC; Granick SColloidal Superstructures Programmed into Magnetic Janus Particles. Adv. Mater2015, 27, 874–879. [PubMed: 25503513]

(16). Aubret A; Youssef M; Sacanna S; Palacci JTargeted Assembly and Synchronization of Self-Spinning Microgears. Nat. Phys2018, 14, 1114–1118.

(17). Grier DGA Revolution in Optical Manipulation. Nature2003, 424, 810–816. [PubMed: 12917694]

(18). Chen Z; Nan F; Yan ZMaking Permanent Optical Matter of Plasmonic Nanoparticles by in Situ Photopolymerization. J. Phys. Chem. C2020, 124, 4215–4220.

(19). Li J; Lin L; Inoue Y; Zheng YOpto-Thermophoretic Tweezers and Assembly. J. Micro Nano-Manuf2018, 6, 040801.

(20). Lin L; Hill EH; Peng X; Zheng YOptothermal Manipulations of Colloidal Particles and Living Cells. Acc. Chem. Res2018, 51, 1465–1474. [PubMed: 29799720]

(21). Pughazhendi A; Chen Z; Wu Z; Li J; Zheng YOpto-Thermoelectric Tweezers: Principles and Applications. Front. Phys2020, 8, 580014.

(22). Lin L; Wang M; Peng X; Lissek EN; Mao Z; Scarabelli L; Adkins E; Coskun S; Unalan HE; Korgel BA; Liz-Marzan LM; Florin EL; Zheng YOpto-Thermoelectric Nanotweezers. Nat. Photonics2018, 12, 195–201. [PubMed: 29785202]

(23). Lin LH; Li JG; Li W; Yogeesh MN; Shi JJ; Peng XL; Liu YR; Rajeeva BB; Becker MF; Liu YY; Akinwande D; Zheng YBOptothermoplasmonic Nanolithography for on-Demand Patterning of 2d Materials. Adv. Funct. Mater2018, 28, 1803990.

(24). Duhr S; Braun DWhy Molecules Move Along a Temperature Gradient. Proc. Natl. Acad. Sci. U. S. A2006, 103, 19678–19682. [PubMed: 17164337]

(25). Reichl M; Herzog M; Gotz A; Braun DWhy Charged Molecules Move across a Temperature Gradient: The Role of Electric Fields. Phys. Rev. Lett2014, 112, 198101. [PubMed: 24877967]

(26). Lin L; Zhang J; Peng X; Wu Z; Coughlan ACH; Mao Z; Bevan MA; Zheng YOpto-Thermophoretic Assembly of Colloidal Matter. Sci. Adv2017, 3, No. e1700458. [PubMed: 28913423]

(27). Li J; Hill EH; Lin L; Zheng YOptical Nanoprinting of Colloidal Particles and Functional Structures. ACS Nano2019, 13, 3783–3795. [PubMed: 30875190]

(28). Peng XL; Li JG; Lin LH; Liu YR; Zheng YBOpto-Thermophoretic Manipulation and Construction of Colloidal Superstructures in Photocurable Hydrogels. ACS Appl. Nano Mater2018, 1, 3998–4004. [PubMed: 31106296]

(29). Lin L; Peng X; Zheng YReconfigurable Opto-Thermo-electric Printing of Colloidal Particles. Chem. Commun2017, 53, 7357–7360.

(30). Yang S-C; Fischer W-J; Yang T-LSize-Controllable Micro-Bubble Generation Using a Nanoimprinted Plasmonic Nanopillar Array Absorber in the near-Infrared Region. Appl. Phys. Lett2016, 108, 183105.

(31). Wang Y; Zaytsev ME; Lajoinie G; The HL; Eijkel JCT; van den Berg A; Versluis M; Weckhuysen BM; Zhang X; Zandvliet HJW; Lohse DGiant and Explosive Plasmonic Bubbles by Delayed Nucleation. Proc. Natl. Acad. Sci. U. S. A2018, 115, 7676–7681. [PubMed: 29997175]

(32). Zhao C; Xie Y; Mao Z; Zhao Y; Rufo J; Yang S; Guo F; Mai JD; Huang TJTheory and Experiment on Particle Trapping and Manipulation *via* Optothermally Generated Bubbles. Lab Chip2014, 14, 384–391. [PubMed: 24276624]

(33). Kotnala A; Kollipara PS; Li J; Zheng YOvercoming Diffusion-Limited Trapping in Nanoaperture Tweezers Using Opto-Thermal-Induced Flow. Nano Lett. 2020, 20, 768–779. [PubMed: 31834809]

(34). Zheng Y; Liu H; Wang Y; Zhu C; Wang S; Cao J; Zhu SAccumulating Microparticles and Direct-Writing Micropatterns Using a Continuous-Wave Laser-Induced Vapor Bubble. Lab Chip2011, 11, 3816–3820. [PubMed: 21956638]

(35). Lin L; Peng X; Mao Z; Li W; Yogeesh MN; Rajeeva BB; Perillo EP; Dunn AK; Akinwande D; Zheng YBubble-Pen Lithography. Nano Lett. 2016, 16, 701–708. [PubMed: 26678845]

(36). Bangalore Rajeeva B; Lin L; Perillo EP; Peng X; Yu WW; Dunn AK; Zheng YHigh-Resolution Bubble Printing of Quantum Dots. ACS Appl. Mater. Interfaces2017, 9, 16725–16733. [PubMed: 28452214]

(37). Rajeeva BB; Alabandi MA; Lin L; Perillo EP; Dunn AK; Zheng YPatterning and Fluorescence Tuning of Quantum Dots with Haptic-Interfaced Bubble Printing. J. Mater. Chem. C2017, 5, 5693–5699.

(38). Rajeeva BB; Wu Z; Briggs A; Acharya PV; Walker SB; Peng X; Bahadur V; Bank SR; Zheng YPoint-and-Shoot" Synthesis of Metallic Ring Arrays and Surface-Enhanced Optical Spectroscopy. Adv. Opt. Mater2018, 6, 1701213.

(39). Rajeeva BB; Kunal P; Kollipara PS; Acharya PV; Joe M; Ide MS; Jarvis K; Liu Y; Bahadur V; Humphrey SM; Zheng YAccumulation-Driven Unified Spatiotemporal Synthesis and Structuring of Immiscible Metallic Nanoalloys. Matter2019, 1, 1606–1617.

(40). Li J; Liu Y; Lin L; Wang M; Jiang T; Guo J; Ding H; Kollipara PS; Inoue Y; Fan D; Korgel BA; Zheng YOptical Nanomanipulation on Solid Substrates via Optothermally-Gated Photon Nudging. Nat. Commun2019, 10, 5672. [PubMed: 31831746]

(41). Nosonovsky MModel for Solid-Liquid and Solid-Solid Friction of Rough Surfaces with Adhesion Hysteresis. J. Chem. Phys2007, 126, 224701. [PubMed: 17581074]

(42). Sharma B; Frontiera RR; Henry A-I; Ringe E; Van Duyne RPSERS: Materials, Applications, and the Future. Mater. Today2012, 15, 16–25.

(43). Lin L; Peng X; Wang M; Scarabelli L; Mao Z; Liz-Marzan LM; Becker MF; Zheng YLight-Directed Reversible Assembly of Plasmonic Nanoparticles Using Plasmon-Enhanced Thermophoresis. ACS Nano2016, 10, 9659–9668. [PubMed: 27640212]

(44). Wang X; Zhang J; Nazzal A; Xiao MPhoto-Oxidation-Enhanced Coupling in Densely Packed Cdse Quantum-Dot Films. Appl. Phys. Lett2003, 83, 162–164.

(45). Lin LH; Lepeshov S; Krasnok A; Jiang TZ; Peng XL; Korgel BA; Alu A; Zheng YBAll-Optical Reconfigurable Chiral Meta-Molecules. Mater. Today2019, 25, 10–20.

(46). Wang Z; Jing L; Yao K; Yang Y; Zheng B; Soukoulis CM; Chen H; Liu YOrigami-Based Reconfigurable Metamaterials for Tunable Chirality. Adv. Mater2017, 29, 1700412.

(47). Ma W; Cheng F; Liu YDeep-Learning-Enabled on-Demand Design of Chiral Metamaterials. ACS Nano2018, 12, 6326–6334. [PubMed: 29856595]

(48). Li J; Wang M; Wu Z; Li H; Hu G; Jiang T; Guo J; Liu Y; Yao K; Chen Z; Fang J; Fan D; Korgel BA; Alù A; Zheng YTunable Chiral Optics in All-Solid-Phase Reconfigurable Dielectric Nanostructures. Nano Lett. 2021, 21, 973–979. [PubMed: 33372805]

(49). Hendry E; Carpy T; Johnston J; Popland M; Mikhaylovskiy RV; Lapthorn AJ; Kelly SM; Barron LD; Gadegaard N; Kadodwala MUltrasensitive Detection and Characterization of Biomolecules Using Superchiral Fields. Nat. Nanotechnol2010, 5, 783–787. [PubMed: 21037572]

(50). Wu Z; Li J; Zhang X; Redwing JM; Zheng YRoom-Temperature Active Modulation of Valley Dynamics in a Monolayer Semiconductor through Chiral Purcell Effects. Adv. Mater2019, 31, No. 1904132.

(51). Wu Z; Zheng YMoiré Chiral Metamaterials. Adv. Opt. Mater2017, 5, 1700034.

(52). Lin L; Peng X; Wei X; Mao Z; Xie C; Zheng YThermophoretic Tweezers for Low-Power and Versatile Manipulation of Biological Cells. ACS Nano2017, 11, 3147–3154. [PubMed: 28230355]

(53). Kotnala A; Zheng YOpto-Thermophoretic Fiber Tweezers. Nanophotonics2019, 8, 475–485. [PubMed: 34290953]

(54). Lin L; Kollipara PS; Kotnala A; Jiang T; Liu Y; Peng X; Korgel BA; Zheng YOpto-Thermoelectric Pulling of Light-Absorbing Particles. Light: Sci. Appl2020, 9, 34. [PubMed: 32194948]

(55). Ndukaife JC; Kildishev AV; Nnanna AGA; Shalaev VM; Wereley ST; Boltasseva ALong-Range and Rapid Transport of Individual Nano-Objects by a Hybrid Electrothermoplasmonic Nanotweezer. Nat. Nanotechnol2016, 11, 53–59. [PubMed: 26524398]

(56). Ndukaife JC; Xuan Y; Nnanna AGA; Kildishev AV; Shalaev VM; Wereley ST; Boltasseva AHigh-Resolution Large-Ensemble Nanoparticle Trapping with Multifunctional Thermoplasmonic Nanohole Metasurface. ACS Nano2018, 12, 5376–5384. [PubMed: 29847087]

(57). Hong C; Yang S; Ndukaife JCStand-Off Trapping and Manipulation of Sub-10 nm Objects and Biomolecules Using Opto-Thermo-Electrohydrodynamic Tweezers. Nat. Nanotechnol2020, 15, 908–913. [PubMed: 32868919]

(58). Nedev S; Urban AS; Lutich AA; Feldmann JOptical Force Stamping Lithography. Nano Lett. 2011, 11, 5066–5070. [PubMed: 21992538]

(59). Gür FN; McPolin CPT; Raza S; Mayer M; Roth DJ; Steiner AM; Löffler M; Fery A; Brongersma ML; Zayats AV; König TAF; Schmidt TLDNA-Assembled Plasmonic Waveguides for Nanoscale Light Propagation to a Fluorescent Nanodiamond. Nano Lett. 2018, 18, 7323–7329. [PubMed: 30339400]

(60). Shi J; Monticone F; Elias S; Wu Y; Ratchford D; Li X; Alu AModular Assembly of Optical Nanocircuits. Nat. Commun2014, 5, 3896. [PubMed: 24871450]

(61). Kruk S; Poddubny A; Smirnova D; Wang L; Slobozhanyuk A; Shorokhov A; Kravchenko I; Luther-Davies B; Kivshar YNonlinear Light Generation in Topological Nanostructures. Nat. Nanotechnol2019, 14, 126–130. [PubMed: 30559485]

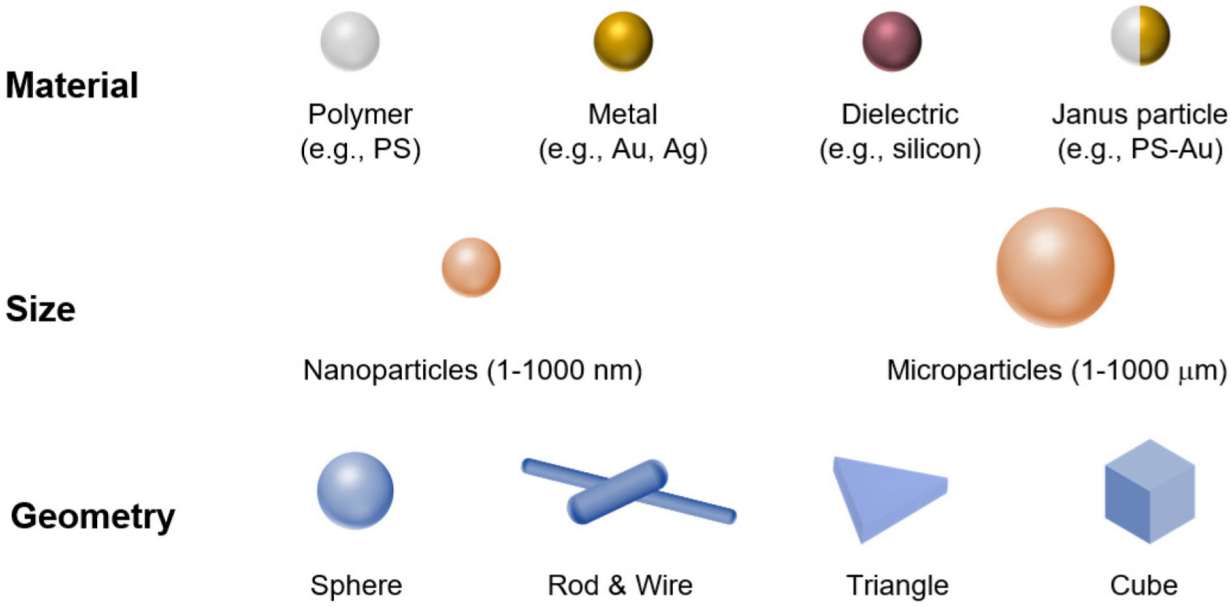

Figure 1.

Schematics of representative colloidal particles as building blocks in the optothermal assembly of superstructures. Chemical synthesis techniques can precisely tune the composition, size, and shape of the diverse building blocks down to the atomic scale.

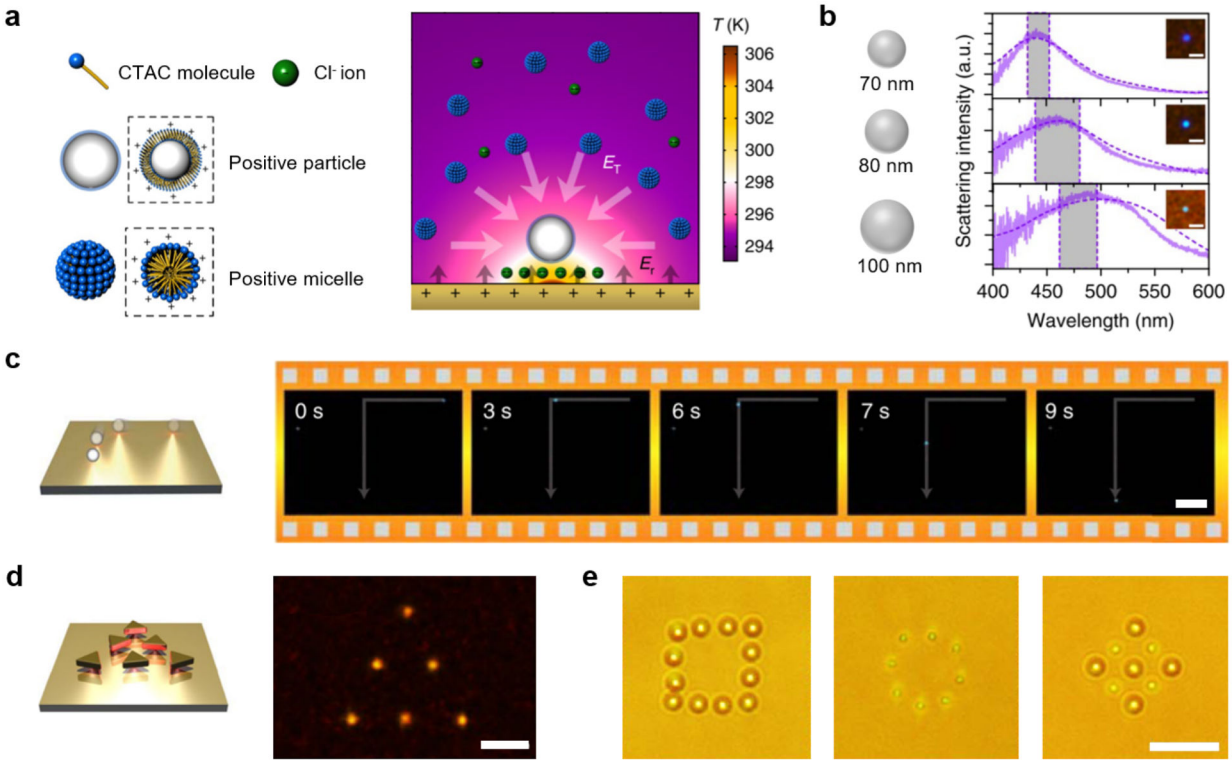

Figure 2.

Opto-thermoelectric tweezers for on-demand trapping and manipulation of colloidal particles as building blocks in optothermal assembly. (a) Schematic of the working principle of opto-thermoelectric tweezers. (b) Dark-field optical images, experimental scattering spectra, and simulated scattering spectra (dashed lines) of the trapped single metal nanoparticles with different sizes. (c) Schematic and successive optical images showing the dynamic manipulation of a single 100 nm silver nanosphere. (d) Parallel trapping of six 150 nm gold nanotriangles. (e) Optical images showing the parallel trapping of PS beads of different sizes. Scale bars: (b) 2 μm, (c) 20 μm, (d) 5 μm, and (e) 10 μm. (a–d) Adapted with permission from ref 22. Copyright 2018 Springer Nature. (e) Adapted with permission from ref 26. Copyright 2017 American Association for the Advancement of Science.

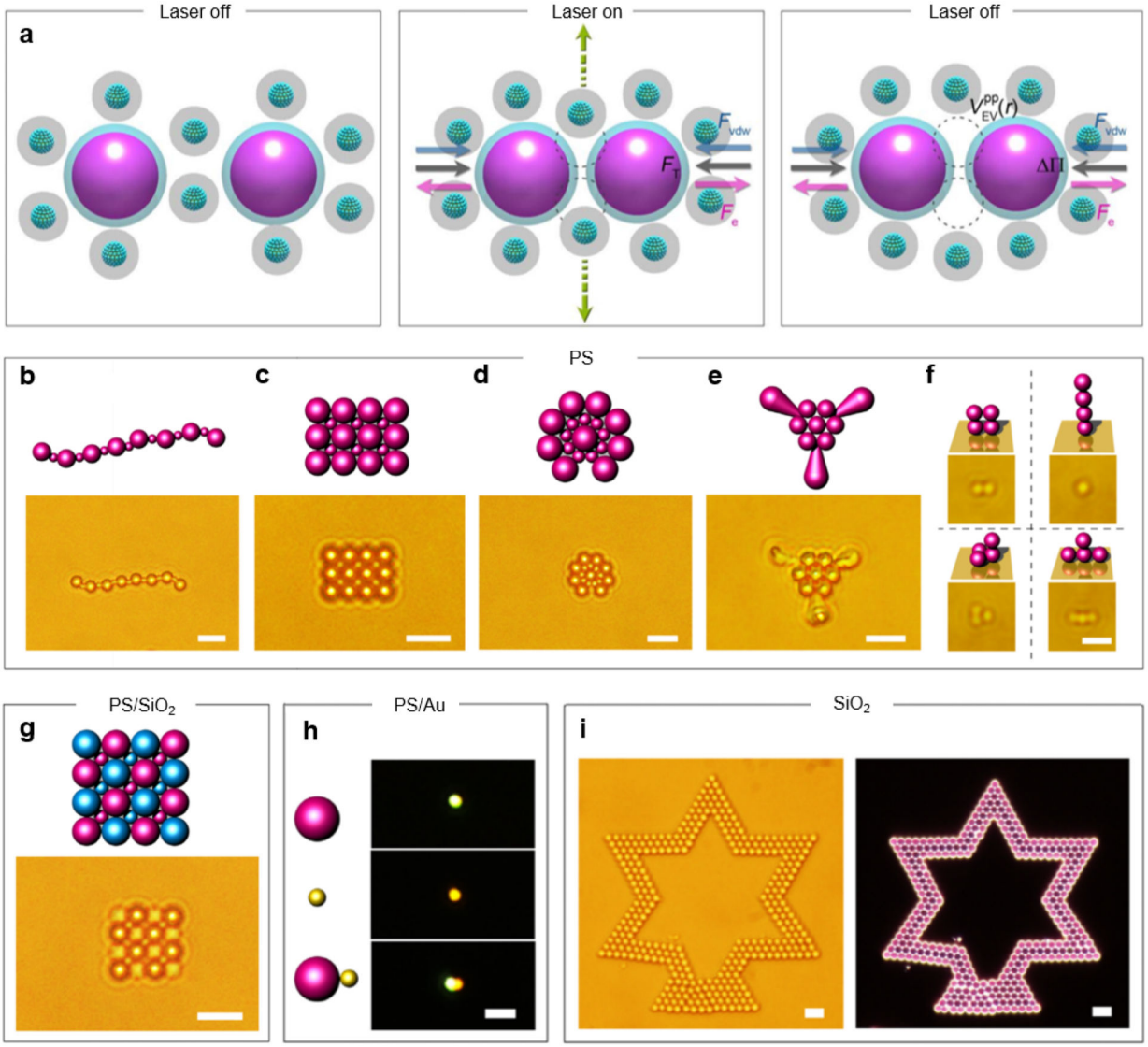

Figure 3.

Opto-thermoelectric assembly of colloidal matter. (a) Schematics of the depletion attraction between two colloidal particles. (b) Assembly of 2 and 0.96 μm PS beads into a 1D chain. (c) 2D assembly of 2 and 0.96 μm PS beads into a hybrid square. (d) 2D hybrid assembly of a double-layer Saturn-ring structure with 2 and 0.96 μm PS beads. (e) 2D hybrid assembly of 2 μm PS beads and anisotropic PS particles. (f) 3D reconfigurable assembly of four 500 nm PS beads. (g) 2D assembly of a heterogeneous superlattice with 2 μm PS, 0.96 μm PS, 2 μm silica, and 1 μm silica beads. (h) Assembly of a dimer with a 500 nm PS bead and a 200 nm Au nanosphere. (i) 2D assembly of a large-area star pattern with 2 μm silica beads. Scale bars: (b–e, g, and i) 5 μm; (f, h) 2 μm. Adapted with permission from ref 26. Copyright 2017 American Association for the Advancement of Science.

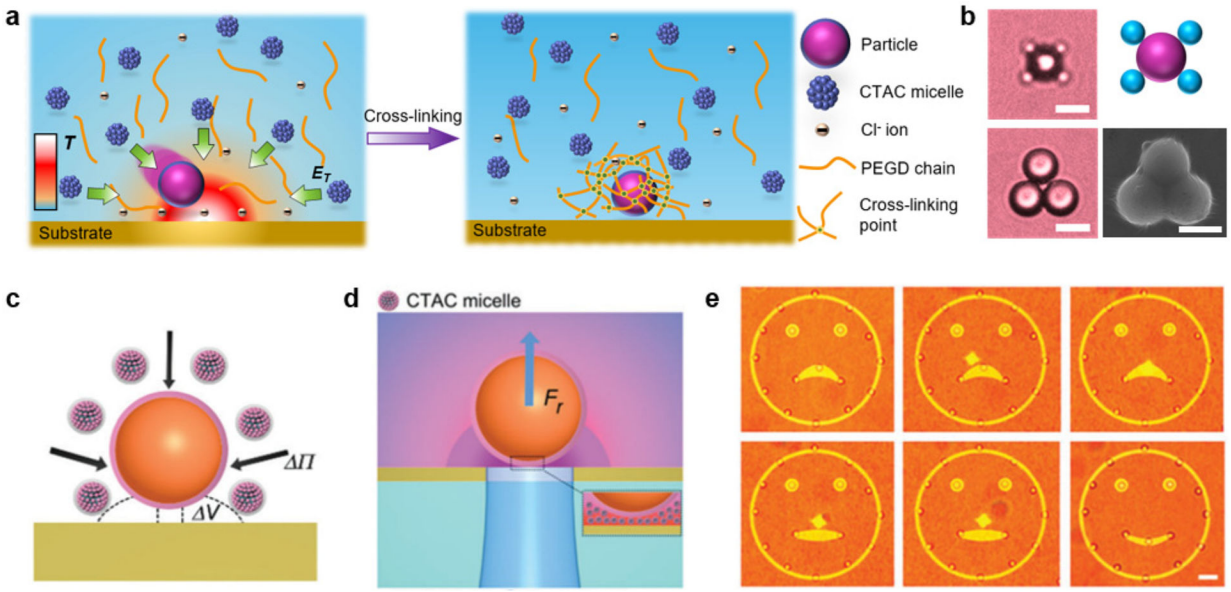

Figure 4.

Opto-thermoelectric printing of colloidal structures. (a) Schematic illustration of the opto-thermoelectric trapping of a colloidal particle in a hydrogel solution and subsequent immobilization of the trapped particle through UV cross-linking. (b) Optical, schematic, and scanning electron microscopy (SEM) images of the examples of the immobilized colloidal structures. (c) Schematic of the CTAC micelle-mediated depletion attraction between the particle and the substrate for opto-thermoelectric printing. (d) Schematic of releasing a printed particle from the substrate by accumulating CTAC micelles in the gap between the particle and the substrate. (e) Optical images of the reconfigurable printing of a “sad-face” pattern into a “smiley-face” pattern with 2 μm PS beads. Scale bars: (b, e) 5 μm. (a, b) Adapted with permission from ref 28. Copyright 2018 American Chemical Society. (c–e) Adapted with permission from ref 29. Copyright 2017 The Royal Society of Chemistry.

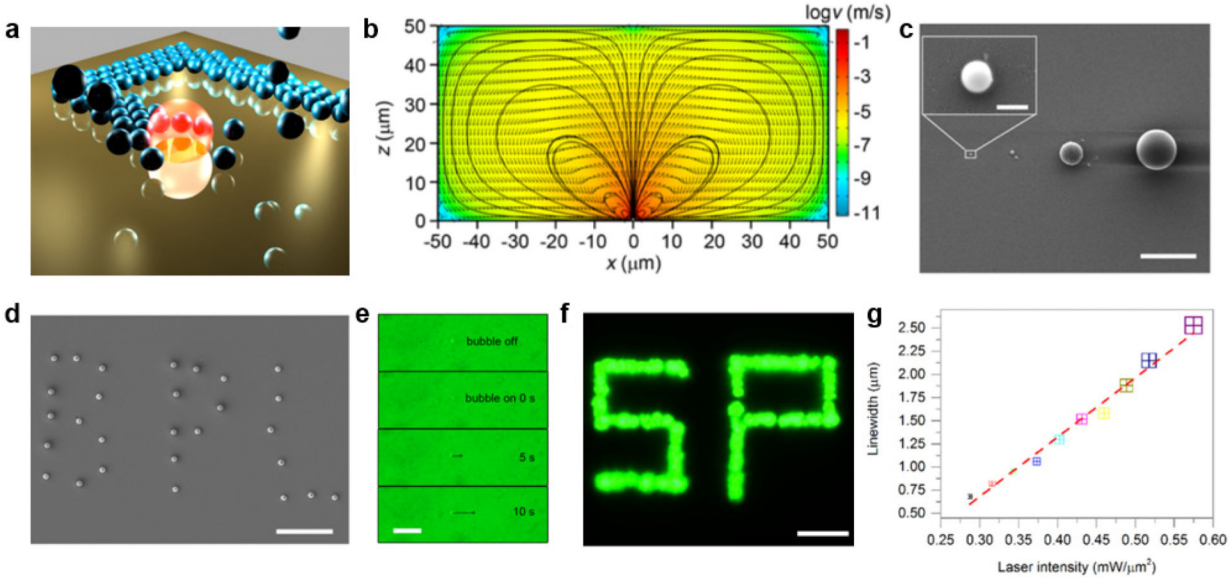

Figure 5.

Working principle and capability of bubble-pen lithography. (a) Schematic of BPL. (b) Simulated convection flow around a 1 μm bubble. (c) Printing single particles with different sizes ranging from 540 nm to 9.51 μm by BPL. (d) SEM image of the BPL pattern of printed 0.96 μm PS beads. (e) Optical images showing the continuous printing of 540 nm PS beads by BPL. (f) Dark-field optical image of the SP pattern of printed 540 nm PS beads. (g) Plot of the width of the continuously printed lines vs the incident laser intensity. Scale bars: (c, d, and f) 10 μm, inset in (c) 500 nm, and (e) 50 μm. (a–f) Adapted with permission from ref 35. Copyright 2016 American Chemical Society. (g) Adapted with permission from ref 36. Copyright 2017 American Chemical Society.

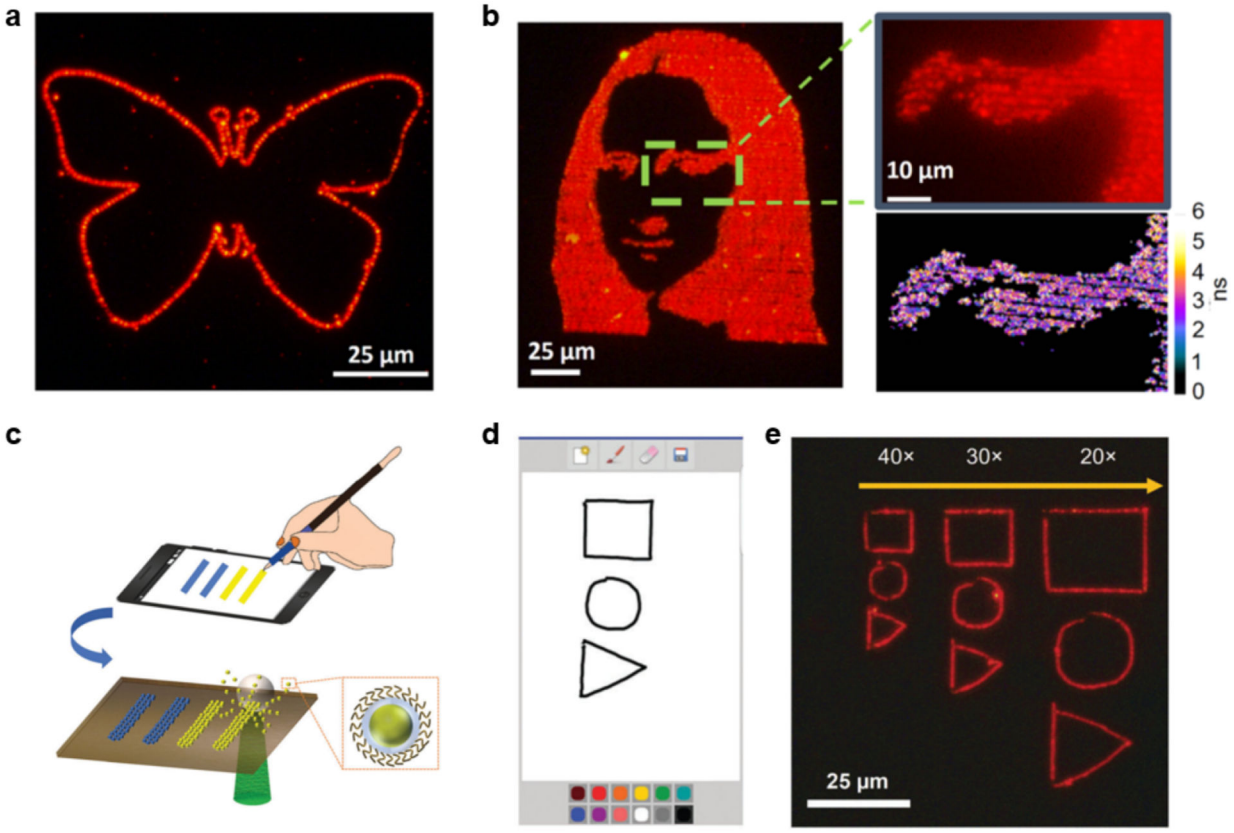

Figure 6.

Bubble printing of quantum dots. (a) Fluorescence image of a butterfly contour consisting of red QDs printed by BPL. The line width is 1 μm. (b) Fluorescent image of the Mona Lisa printed with red QDs using a raster scanning approach. The magnified fluorescent image along with fluorescence lifetime mapping shows the high-resolution, high-density, and uniform patterning capability of BPL. (c) Schematic of haptic-interfaced BPL. (d) Snapshot showing the basic shapes drawn on the smartphone screen. (e) Printing of the pattern in (d) with red QDs at different downscaling factors via haptic-interfaced BPL. (a, b) Adapted with permission from ref 36. Copyright 2017 American Chemical Society. (c–e) Adapted with permission from ref 37. Copyright 2017 The Royal Society of Chemistry.

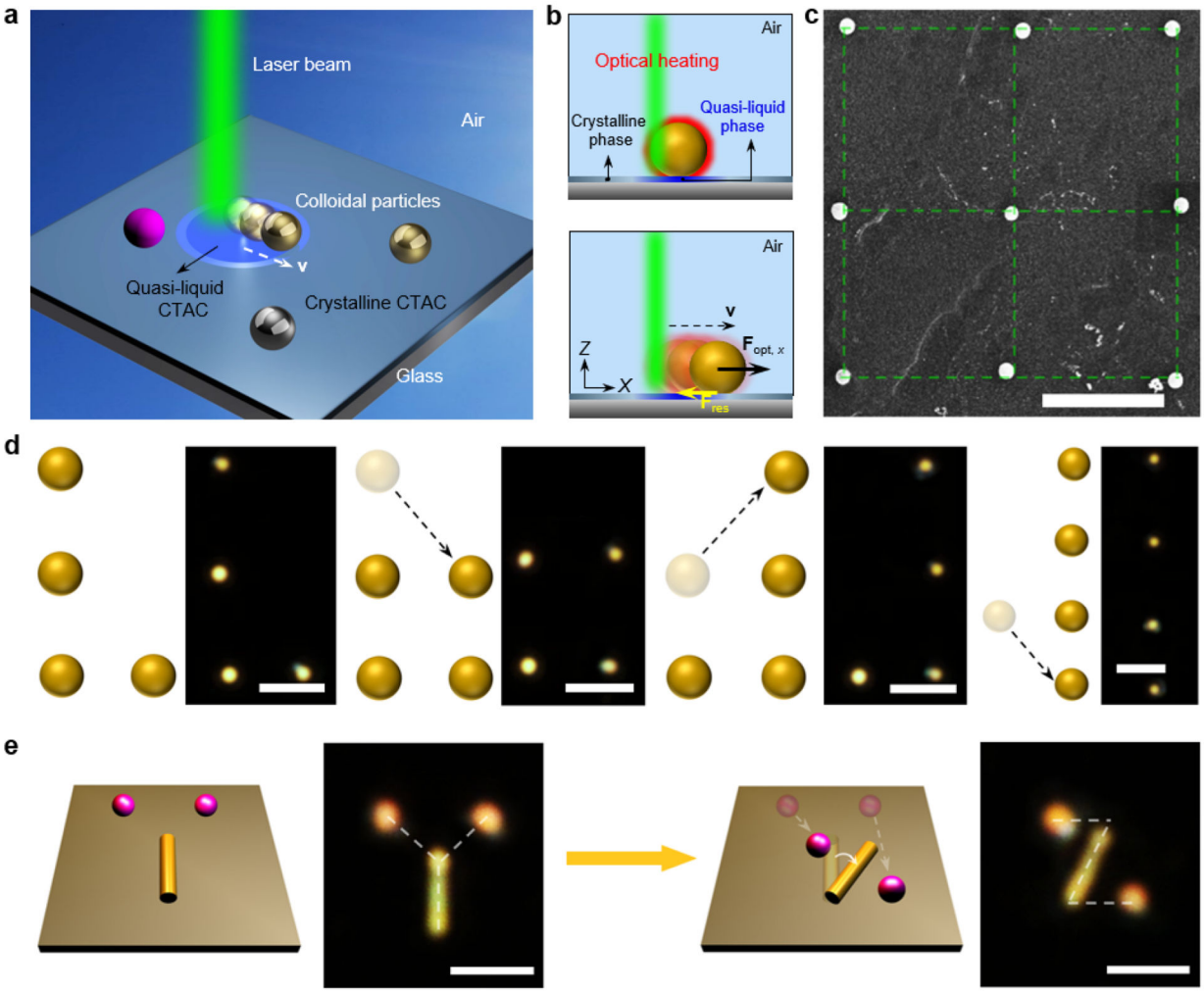

Figure 7.

Optothermally-gated photon nudging. (a) Schematic illustration of OPN on a solid substrate. (b) Working mechanism of OPN based on the synergy of optical heating and optical scattering forces. (c) SEM image of a 2D assembly of 500 nm silicon nanoparticles into a 3 × 3 array. (d) Reconfigurable assembly of four 300 nm gold nanoparticles. Four particles were sequentially arranged into an L shape, a square, a mirrored L shape, and a straight line. The dashed arrows show the reconfigurable patterning sequence. (e) Reconfigurable assembly of metal–dielectric hybrid nanostructures. Two 500 nm silicon nanoparticles and one gold nanowire were sequentially patterned into “Y” and “Z”. Scale bars: (c, d) 5 μm and (e) 3 μm. Adapted with permission from ref 40. Copyright 2019 Springer Nature.

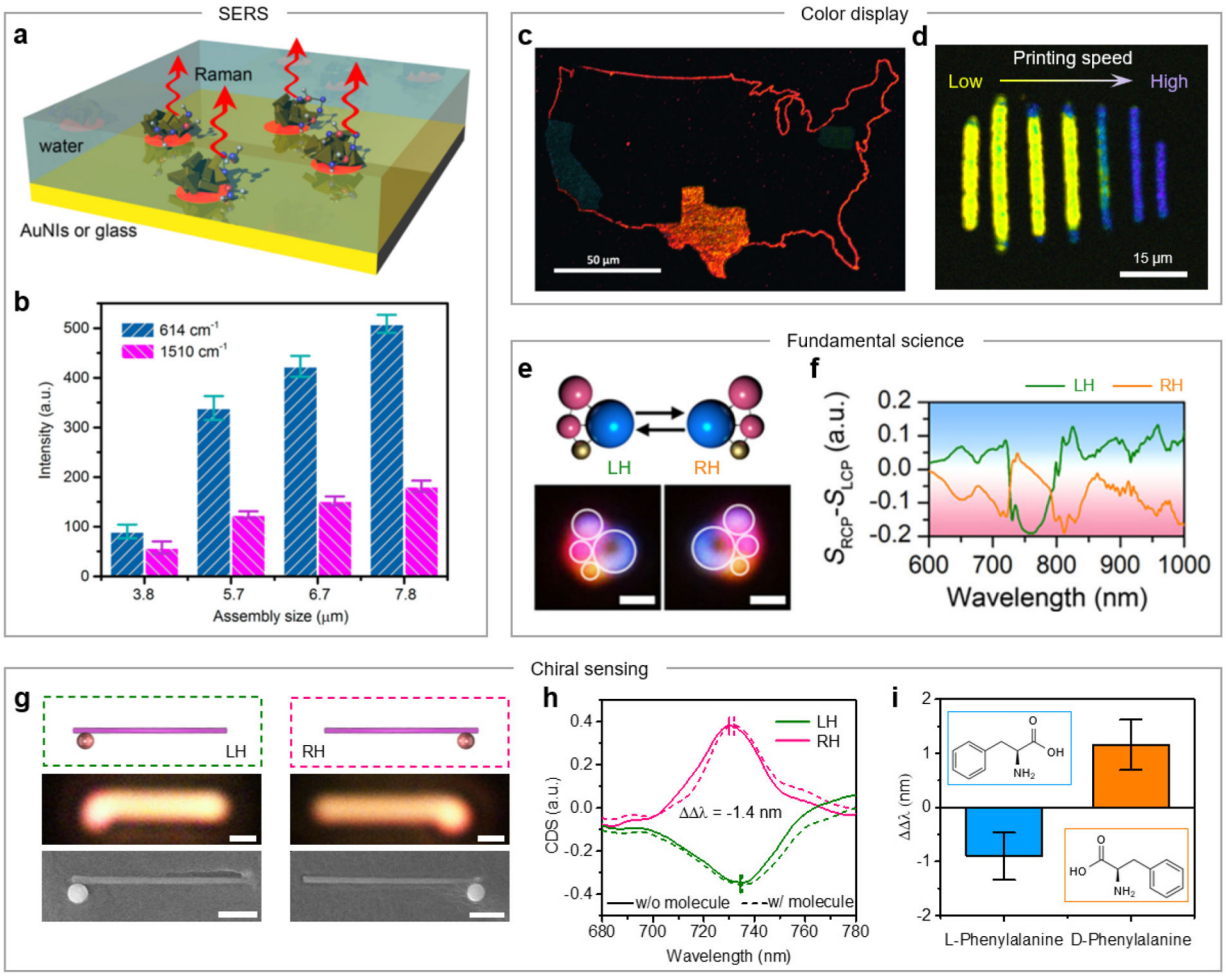

Figure 8.

Applications of optothermally assembled nanostructures. (a) Schematics of the nanoparticle assemblies for multiplex in situ SERS. (b) Assembly-size-dependent SERS intensities of rhodamine 6G based on the assemblies of golf nanotriangles. (c) A U.S. map with the states of Texas, California, and Pennsylvania printed with different QDs. (d) Fluorescent image of the patterns of yellow QDs printed by haptic-interfaced BPL. The printing speed decreases from left to right, which is controlled by the hand movement speed. (e) Schematic and optical images of the chiral metamolecules composed of a 1 μm PS bead, a 400 nm gold nanoparticle, a 500 nm silicon nanoparticle, and a 700 nm silicon nanoparticle. (f) Circular differential scattering (CDS) spectra of the chiral metamolecules in (e). (g) Schematic, optical, and SEM images of the assembled LH and RH chiral nanostructures with a silicon nanoparticle and a silicon nanowire. (h) CDS spectra of the LH and RH structures before and after the adsorption of L-phenylalanine. (i) $\Delta\Delta\lambda$ values for L-phenylalanine and D-phenylalanine with opposite signs. Insets show the chemical structures of the chiral molecules. Scale bars: (e, g) 1 μm. (a, b) Adapted with permission from ref 43. Copyright 2016 American Chemical Society. (c) Adapted with permission from ref 36. Copyright 2017 American Chemical Society. (d) Adapted with permission from ref 37. Copyright 2017 The Royal Society of Chemistry. (e, f) Adapted with permission from ref 45. Copyright 2019

Elsevier. (g–i) Adapted with permission from ref 48. Copyright 2021 American Chemical Society.

Table 1.

Summary and Comparison of Three Optothermal Assembly Techniques

techniques	mechanism	applicable compositions	sizes of assemblies	reconfigurability of assemblies	working environments	optical intensities	throughput	additional notes
opto-thermoelectric assembly (OTA)	thermoelectricity and depletion	all	suitable for small scale (<100 μm)	yes	specific solutions	0.05−0.4 mW/μm^2	low	additional steps required to immobilize the assembled structures on substrates
bubble-pen lithography (BPL)	Marangoni and natural convections	all	up to cm scale	no	any solutions	0.5−5 mW/μm^2	high	relatively lower spatial precision of particles due to the microscale of bubbles
optothermally-gated photon nudging (OPN)	heat-induced phase transition and optical scattering force	materials with strong light scattering	suitable for small scale (<100 μm)	yes	any solid substrates	0.2−5 mW/μm^2	low	no Brownian motion during the assembly